

# The equation of state of two dimensional Yang-Mills theory

Nikhil Karthik\* and Rajamani Narayanan†

*Department of Physics, Florida International University, Miami, FL 33199.*

## Abstract

We study the pressure,  $P$ , of  $SU(N)$  gauge theory on a two-dimensional torus as a function of area,  $A = l/t$ . We find a cross-over scale that separates the system on a large circle from a system on a small circle at any finite temperature. The cross-over scale approaches zero with increasing  $N$  and the cross-over becomes a first order transition as  $N \rightarrow \infty$  and  $l \rightarrow 0$  with the limiting value of  $\frac{2Pl}{(N-1)t}$  depending on the fixed value of  $Nl$ .

arXiv:1411.2477v1 [hep-th] 10 Nov 2014

---

\*Electronic address: nkarthik@fiu.edu

†Electronic address: rajamani.narayanan@fiu.edu

## I. INTRODUCTION

The partition function for  $SU(N)$  gauge theory on a 2d torus with spatial extent  $l$  and temperature  $t$  is only a function of the area,  $A = l/t$ , and is given by [1]

$$Z_N(A) = \sum_r \exp\left(-\frac{C_r^{(2)}l}{Nt}\right), \quad (1)$$

where  $C_r^{(2)}$  is the value of Casimir in the representation  $r$ . One can arrive at (1) by taking the continuum limit of a lattice formalism on a finite lattice [2]. The asymptotic behavior at large  $N$  was studied in [3] where only representations with  $C_r^{(2)}$  of  $\mathcal{O}(N)$  dominate. Since the partition function is a sum over string like states with energies proportional to the spatial extent,  $l$ , the pressure given by

$$P \equiv t \frac{\partial}{\partial l} \ln Z = \frac{\partial}{\partial A} \ln Z = -\frac{1}{N} \langle C_r^{(2)} \rangle, \quad (2)$$

is negative.

The partition function for  $SU(2)$  is simple and given by

$$Z = \sum_{\lambda=0}^{\infty} e^{-\frac{(\lambda^2+2\lambda)A}{4}} = \frac{1}{2} e^{\frac{A}{4}} \left[ \sum_{\lambda=-\infty}^{\infty} e^{-\frac{\lambda^2 A}{4}} - 1 \right] = \frac{1}{2} e^{\frac{A}{4}} \left[ \sqrt{\frac{4\pi}{A}} \sum_{\lambda=-\infty}^{\infty} e^{-\frac{4\pi^2 \lambda^2}{A}} - 1 \right]. \quad (3)$$

The asymptotic behavior of the equation of state is

$$\frac{Pl}{t} = -\frac{3l}{4t} e^{-\frac{3l}{4t}} \quad \text{as } l \rightarrow \infty, \quad (4)$$

and

$$\frac{Pl}{t} = -\frac{1}{2} \quad \text{as } l \rightarrow 0. \quad (5)$$

The behavior at large  $l$  is dominated by a few low lying energy states where as the behavior at small  $l$  comes from a sum over all states and could be interpreted as the equipartition limit with the number of degrees of freedom being 1 for  $SU(2)$ . The cross-over from the behavior on a large circle to a small circle is shown in Figure 1.

Expecting that the equipartition limit is given by

$$\frac{Pl}{t} = -\frac{N-1}{2} \quad \text{as } l \rightarrow 0, \quad (6)$$

for all  $N$ , we define

$$Q(\alpha) \equiv -\frac{2Pl}{(N-1)t}; \quad \text{with } \alpha = \frac{Nl}{t}, \quad (7)$$

and study this quantity in this paper.

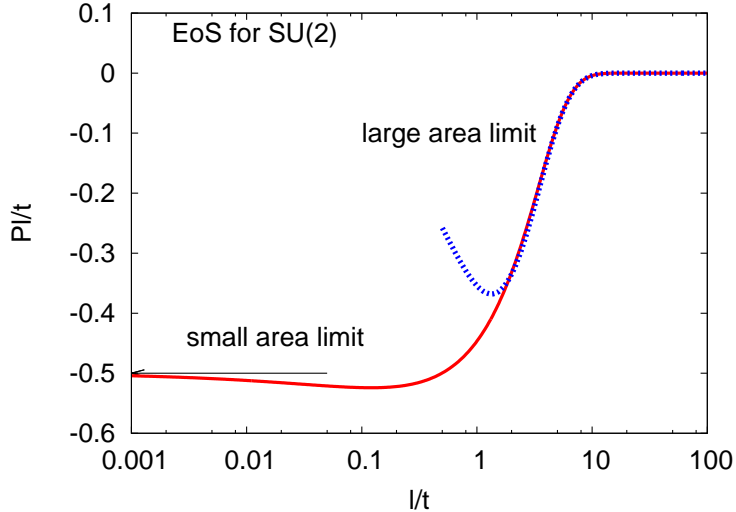


FIG. 1: The equation of state for SU(2) gauge theory on a two-dimensional torus is shown as the solid curve. The asymptotic values of  $Pl/t$  at small area is -0.5. At very large area,  $Pl/t$  behaves as  $0.75 \exp(-0.75l/t)l/t$ , which is shown as the dotted curve. There is a cross-over between the two limits.

## II. SUMMARY OF RESULTS

We will show the following results in this paper using a numerical simulation of the partition function in Eq. (1):

1.  $Q(\alpha)$  falls on a universal curve as  $N \rightarrow \infty$ .
2.  $Q(\alpha)$  goes to zero as  $\alpha$  goes to infinity. This result implies that the pressure at infinite  $N$  is zero for all  $l$  at any  $t$  as long as one takes  $N \rightarrow \infty$  keeping  $l$  and  $t$  finite and is consistent with physics being independent of temperature and spatial extent in the infinite  $N$  limit [4, 5].
3.  $Q(\alpha)$  goes to unity as  $\alpha$  goes to zero. This limit is reached from a finite  $l$  and  $t$  only at finite  $N$ .
4. There is a cross-over point defined as a peak in the susceptibility,

$$\chi = A \frac{\partial}{\partial A} Q = \alpha \frac{\partial}{\partial \alpha} Q. \quad (8)$$

(a) The large  $l$  side of the cross-over is dominated by representations where  $C_r^{(2)}$  are of  $\mathcal{O}(N)$ . This is the case of interest for all non-zero  $l$  at infinite  $N$  and studied in [3].

(b) The small  $l$  side of the cross-over is dominated by representations where  $C_r^{(2)}$  are of  $\mathcal{O}(N^2)$ .

5. Since the value of  $Q$  at infinite  $N$  and  $l = 0$  (or equivalently  $t = \infty$ ) depends on the approach to the limit,  $N \rightarrow \infty$  and  $l \rightarrow 0$ , there is a first order transition confirming the argument in [6].

### III. PROPERTIES OF CASIMIR FOR SU(N)

The representations of  $SU(N)$  are specified by the sequence of integers  $\Lambda_r = (\lambda_1, \lambda_2, \dots, \lambda_{N-1})$ , subjected to the ordering  $\lambda_i \geq \lambda_{i+1}$  and the value of  $C_r^{(2)}$  is

$$C_r^{(2)} = \sum_{i=1}^{N-1} \lambda_i^2 - \sum_{i=1}^{N-1} i\lambda_i - \frac{\lambda^2}{N} + (N+1)\lambda \quad \text{where} \quad \lambda = \sum_{i=1}^{N-1} \lambda_i. \quad (9)$$

The maximum and the minimum value of Casimir, given the constraint that  $\lambda$  has to be kept fixed, would be used in the subsequent sections. The representation with the maximum value of  $C_r^{(2)}$  for a given  $\lambda$  is given by

$$\Lambda_{\max} = (\lambda, 0, \dots, 0). \quad (10)$$

The minimum value of  $C_r^{(2)}$  is given by the sequence  $\Lambda_{\min}$ :

$$\lambda_i = \begin{cases} \lfloor \frac{\lambda}{N-1} \rfloor + 1 & \text{if } i \leq k \equiv \lambda - (N-1)\lfloor \frac{\lambda}{N-1} \rfloor \\ \lfloor \frac{\lambda}{N-1} \rfloor & \text{if } i > k. \end{cases} \quad (11)$$

To prove that the two sequences extremize the Casimir, note that the Casimir decreases under the transformation  $(\lambda_1, \lambda_2, \dots, \lambda_i, \dots, \lambda_j, \dots, \lambda_{N-1})$  to  $(\lambda_1, \lambda_2, \dots, \lambda_i - 1, \dots, \lambda_j + 1, \dots, \lambda_{N-1})$  for  $j > i$ , provided this transformation is allowed. Such a transformation is not possible for  $\Lambda_{\min}$ . Similarly, the reverse of that transformation is not possible on  $\Lambda_{\max}$ . One can prove by contradiction that  $\Lambda_{\min}$  and  $\Lambda_{\max}$  are unique to satisfy these properties.

We have shown the behaviour of the maximum and the minimum value of  $C_r^{(2)}$  as a function of  $\lambda$  in Figure 2. The minimum of  $C_r^{(2)}$  shows a quasi-periodic behaviour, with

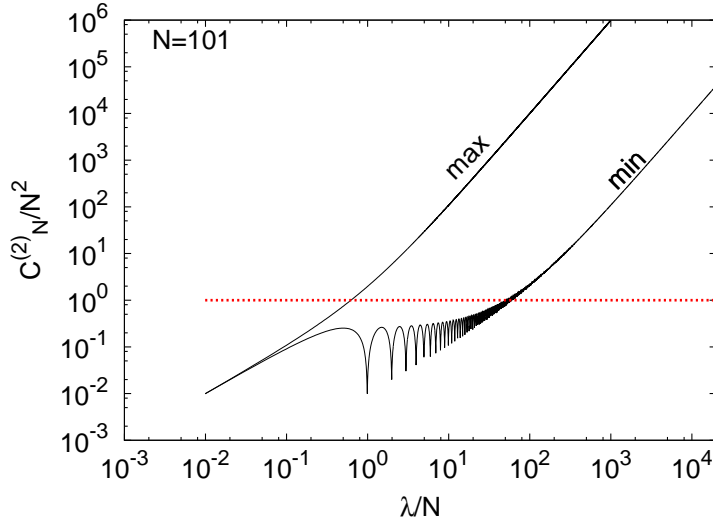


FIG. 2: Behaviour of Casimir as a function of  $\lambda$ . The upper solid curve is the maximum value of Casimir given a value of  $\lambda$ , as a function of  $\lambda$ . Similarly, the lower solid curve is the minimum value of Casimir given a value of  $\lambda$ , as a function of  $\lambda$ . The dotted line is where  $C_r^{(2)} = N^2$ .

troughs at  $\lambda = qN$  for integer  $q$ . The values of Casimir at these troughs are

$$C_{\min} = N \left( 1 + \left\lfloor \frac{q}{N-1} \right\rfloor \right) \left( 2q - \left\lfloor \frac{q}{N-1} \right\rfloor (N-1) \right), \quad (12)$$

whose dependence on  $N$  is linear for  $q$  between two multiples of  $(N-1)$  and is quadratic for  $q$  that are multiples of  $(N-1)$ . On very large circles (or at very low temperatures), one would expect that only the excitations around these troughs at small  $q$  would be important. On very small circles (or at very high temperatures), large values of  $q$  would become accessible, where all possible Casimir are  $\mathcal{O}(N^2)$ . This is the region above the red dotted line in Figure 2 where  $C_r^{(2)}$  is larger than  $N^2$ . Qualitatively, this is the difference one might expect between the low and high temperature phases.

#### IV. HEAT-BATH ALGORITHM

We simulated the partition function in Eq. (1) by updating  $\Lambda_r$  by the heat-bath algorithm. Each heat-bath update is a sequence of local updates from  $\lambda_1$  to  $\lambda_{N-1}$ , in that order, such that the ordering of  $\lambda_i$  is preserved. For the local update of  $\lambda_i$ , the probability distribution

of  $\lambda_i$  is given by a discrete version of the Gaussian distribution

$$T(\lambda_i) \propto e^{-(\lambda_i - \mu_i)^2 / 2\sigma^2}, \quad (13)$$

subject to the condition  $\lambda_{i+1} \leq \lambda_i \leq \lambda_{i-1}$  for  $i > 1$  and  $\lambda_2 \leq \lambda_1$ . The  $\mu_i$  and  $\sigma_i$  for the above discrete Gaussian distribution are functions of the rest of the  $\lambda_i$ 's forming the heat-bath:

$$\mu_i = \frac{\bar{\lambda} + N \left( \frac{2i - N - 1}{2} \right)}{N - 1} \quad \text{and} \quad \sigma^2 = \frac{N^2}{2A(N - 1)}, \quad (14)$$

where  $\bar{\lambda} = \sum_{j \neq i} \lambda_j$ . For  $i > 1$ , the set of allowed values for  $\lambda_i$  is bounded from above and below. Hence, we included all the allowed possibilities weighted by Eq. (13) as candidates for the update. Since Eq. (14), along with the inequality  $\lambda - \lambda_1 < (N - 2)\lambda_2$ , implies that  $\mu_1 < \lambda_2$ , the probability for  $\lambda_1$  is a monotonically decreasing function. This enables one to put an upper cut-off on  $\lambda_1$ . In our calculation, we used an upper cut-off of  $\lambda_2 + 3\sigma$ . We also checked that changing this value to  $\lambda_2 + 10\sigma$  does not cause any statistically significant changes. Since a representation  $r$  and its conjugate representation  $\bar{r}$  have the same Casimir, one can do an over-relaxation step by a global update  $\lambda'_i = \lambda_1 - \lambda_{N-i+1}$ .

In our simulations, the successive measurements were separated by 100 iterations of 2 heat-bath and 1 over-relaxation steps. The first 2000 measurements were discarded for thermalization. In this way, we collected  $10^4$  configurations of  $\Lambda_r$  at all area and  $N$ .

## V. RESULTS

In the top panel of Figure 3, we show the behaviour of  $Q$  as a function of the scaled area  $\alpha$  for various values of  $N$ . The important thing to notice is that  $Q$  has a large- $N$  limit when plotted as a function of  $\alpha$ . For  $\alpha \ll 1$ ,  $Q$  seems to approach 1 for all  $N$ . This is in agreement with our intuition based on the equipartition theorem. The non-trivial observation is that this cross-over to the equipartition limit happens at a finite value of  $\alpha$  in the large- $N$  limit. For  $\alpha \gg 1$ ,  $Q$  seems to behave as  $N^{-1} \exp(-\sigma\alpha/N)$  for a constant  $\sigma \approx 0.81$  in the large- $N$  limit. This is shown in the bottom panel of Figure 3. Thus, it can also be seen as a cross-over from strong-coupling regime, which has a scale  $\sigma$ , to the weak-coupling regime with no underlying scale.

We determined the cross-over point  $\alpha_c$  using the peak-position of the susceptibility  $\chi$ , after interpolating using multi-histogram reweighting. We show  $\chi$  as a function of  $\alpha$  in

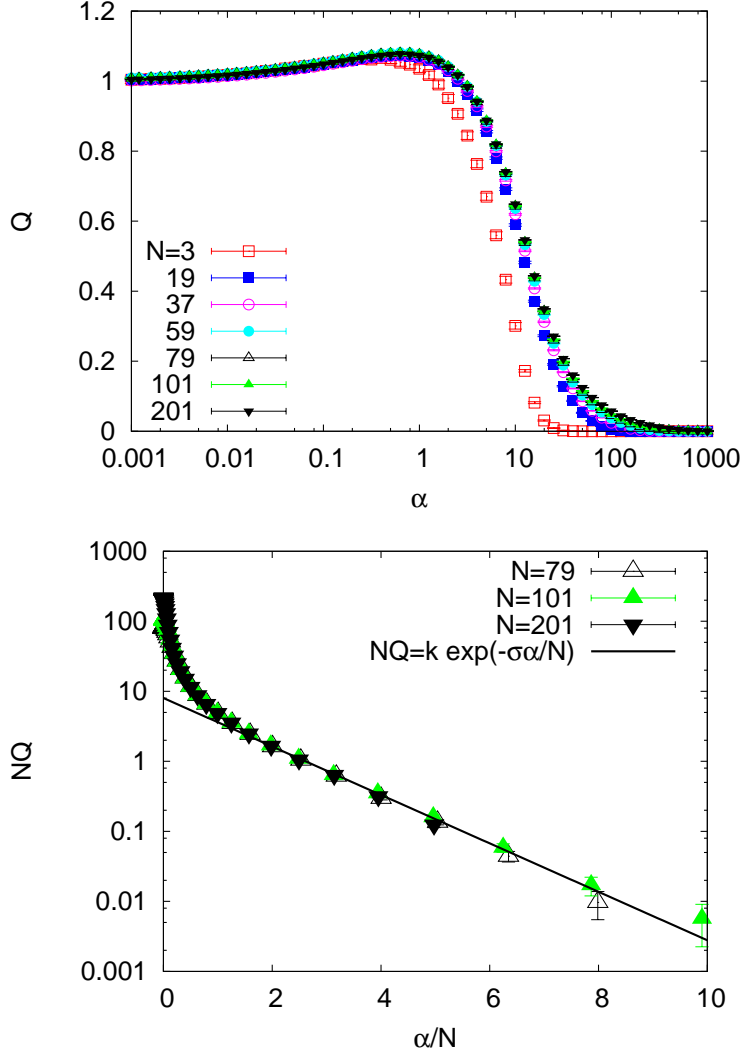


FIG. 3:  $Q$  as a function of the scaled area  $\alpha = NA$  is shown in the top panel. It is seen that  $Q$  as a function of  $\alpha$  has a large- $N$  limit. For very small values of  $\alpha$ ,  $Q$  approaches 1. In the bottom panel, the large area behaviour of  $Q$  in the large- $N$  limit is shown. In this case,  $QN$  behaves as  $\exp(-\sigma\alpha/N)$ .

Figure 4 for various  $N$ . The susceptibility also has a large- $N$  limit when plotted as a function of  $\alpha$ . The peak positions of susceptibility for  $N > 19$  agree within errors, giving us an estimate  $\alpha_c = 12.1(2)$ . This implies that the cross-over area  $A_c = \alpha_c/N$  shifts to smaller values at larger  $N$ . The width of the susceptibility when expressed in terms of the area  $A$  decreases inversely as  $N$ . This is characteristic of finite volume scaling near a first order phase transition, with the large- $N$  limit replacing the thermodynamic limit in this case.

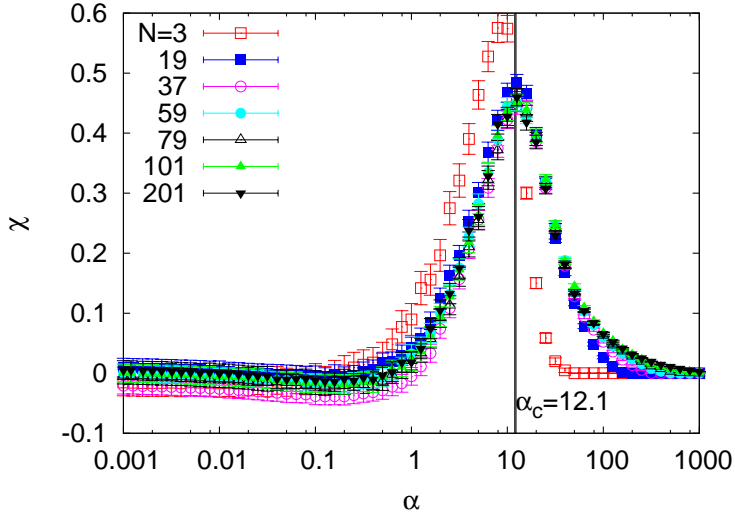


FIG. 4: Susceptibility  $\chi$  as a function of the scaled area  $\alpha = NA$ . The cross-over coupling  $\alpha_c$  is shown by the vertical line.

The reason for this cross-over can be understood from the scatter plot of  $C_r^{(2)}$  versus  $\lambda$  measured during the course of the Monte Carlo run using a value of  $\alpha$ . Such scatter plots at various  $\alpha$  are shown in Figure 5 for two different  $N$ . We also show the maximum and minimum value of Casimir at a fixed  $\lambda$ , as a function of  $\lambda$ . As discussed earlier, the minimum Casimir shows a quasi-periodic behaviour forming wells with a periodicity  $N$ . At large values of  $\alpha$ , the representations near the troughs of these wells at small values of  $\lambda$  get populated. The representations within these wells are sparse, and this discreteness governs the large area behaviour. At very small area, the most probable  $C_r^{(2)}$  moves away from the line of minimum  $C_r^{(2)}$  and remains in a region where one can approximate the distribution of Casimir by a continuum. The cross-over between the two behaviours is what shows up as a peak in  $\chi$ . As discussed in Section III, the Casimir near the troughs at small  $\lambda$  is of  $\mathcal{O}(N)$ , while the Casimir at very large  $\lambda$  is of  $\mathcal{O}(N^2)$ . As shown by the dotted line in Figure 5, this cross-over at  $\alpha \approx 12.1$  roughly occurs when the dominant behaviour  $C_r^{(2)}$  changes from  $\mathcal{O}(N)$  to  $\mathcal{O}(N^2)$ .



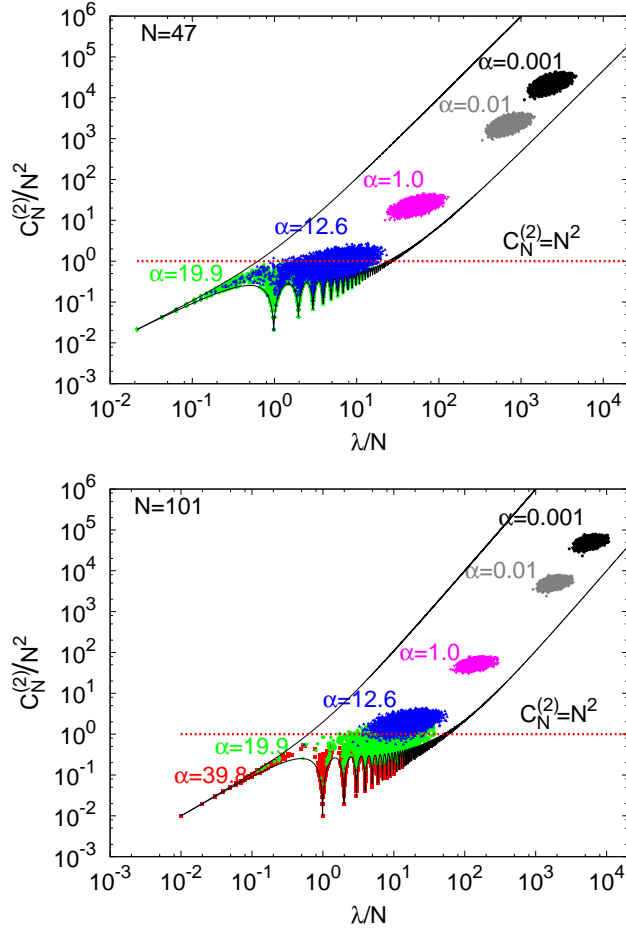


FIG. 5: Scatter plot of  $C_r^{(2)}/N^2$  versus  $\lambda/N$  at various area  $A$ . The top panel is for  $N = 47$  and the bottom one for  $N = 101$ . Each point corresponds to a  $C_r^{(2)}$  and  $\lambda$  measured in the course of Monte Carlo simulation at a particular  $\alpha$  specified by the color. The upper and lower solid curves are the maximum and the minimum value of  $C_r^{(2)}$  at a given  $\lambda$  respectively.

## VI. CONCLUSIONS

Yang-Mills theory in two dimensions is always in the confined phase. We focused on the quantity,  $Q = -\frac{2Pl}{(N-1)t}$ , to study the equation of state. We showed that the equation of state shows a cross-over from strong coupling (large spatial extent) to weak coupling (small spatial extent) within the confined phase. Viewed as a function of  $\alpha = \frac{lN}{t}$ ,  $Q(\alpha)$  approaches a universal curve as  $N \rightarrow \infty$  as shown in Figure 6. This behavior is similar to the Durhuus-Olesen transition [7, 8] with the double scaling limit for the equation of state being  $N \rightarrow \infty$  and  $l \rightarrow 0$  (or  $t \rightarrow \infty$ ) keeping  $\alpha = \frac{lN}{t}$  fixed. There is a line of cross-over,  $\frac{lN}{t} = \alpha_c$ , extending

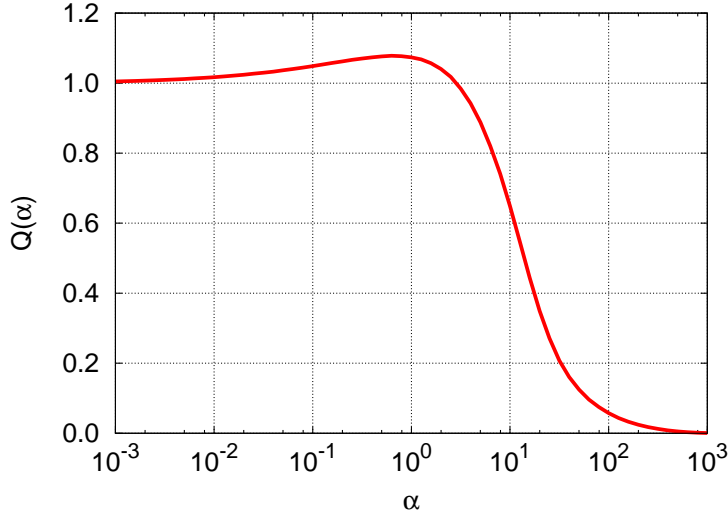


FIG. 6: The large- $N$  limit of  $Q$  as a function of  $\alpha$ .

from the origin in the  $\frac{l}{t} - \frac{1}{N}$  diagram as shown in Figure 7. Well above this line,  $Q \ll 1$  and it behaves as  $\exp(-\sigma A)/N$ . Well below this line,  $Q$  is approximately 1. Depending on the slope,  $\alpha$ , of the line along which the  $N \rightarrow \infty$  and  $\frac{l}{t} \rightarrow 0$  limit is taken, the limiting value of  $Q$  differs. Specifically, if  $N \rightarrow \infty$  limit is taken after the  $A \rightarrow 0$  limit is taken, then  $Q$  is 1. When the two limits are reversed,  $Q$  becomes 0. Therefore, the cross-over along  $AN = \alpha_c$  becomes a first order transition at vanishing area in the large- $N$  limit.

The equation of state in four dimensional Yang-Mills theories for several different values of  $N$  has been recently studied [9]. The pressure is found to be close to zero in the confined phase. In light of this paper, it would be interesting to perform a careful study of the equation of state in the confined phase in three and four dimensions and see if one can see a cross-over similar to the one seen here in two dimensions.

### Acknowledgments

The authors acknowledge partial support by the NSF under grant number PHY-1205396.

---

[1] A. A. Migdal, *Sov.Phys.JETP* **42**, 413 (1975).

[2] J. Kiskis, R. Narayanan, and D. Sigdel, *Phys.Rev.* **D89**, 085031 (2014), 1403.1770.

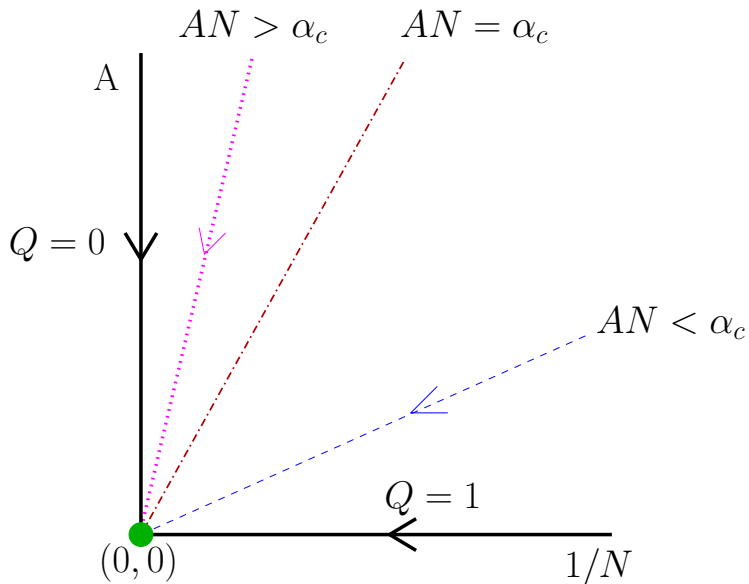


FIG. 7: Phase diagram. Various approaches to vanishing area at large- $N$  are indicated by lines with arrows. The critical value of the slope  $AN = \alpha_c$  is shown as the dot-dashed line. For values of  $AN \gg \alpha_c$  (the dotted line),  $Q$  decays exponentially with area. For values of  $AN \ll \alpha_c$  (the dashed line),  $Q \approx 1$ . In particular, when  $A$  is reduced to 0 after taking the large- $N$  limit (*i.e.*, along  $y$ -axis),  $Q$  vanishes. When the two limits are interchanged (*i.e.*, along  $x$ -axis),  $Q$  becomes 1.

[3] D. J. Gross and W. Taylor, Nucl.Phys. **B400**, 181 (1993), hep-th/9301068.

[4] D. Gross and E. Witten, Phys.Rev. **D21**, 446 (1980).

[5] T. Eguchi and H. Kawai, Phys.Rev.Lett. **48**, 1063 (1982).

[6] L. D. McLerran and A. Sen, Phys.Rev. **D32**, 2794 (1985).

[7] B. Durhuus and P. Olesen, Nucl.Phys. **B184**, 461 (1981).

[8] R. Narayanan and H. Neuberger, JHEP **0712**, 066 (2007), 0711.4551.

[9] S. Datta and S. Gupta, Phys.Rev. **D82**, 114505 (2010), 1006.0938.